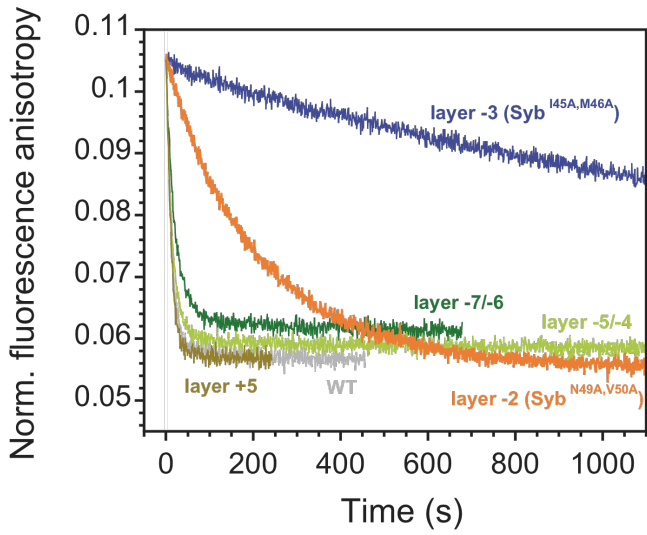


## **Supplementary information**

### **A coiled-coil nucleation site is essential for rapid binding of synaptobrevin to the SNARE acceptor complex**

Katrin Wiederhold, Tobias H. Kloepper, Alexander M. Walter, Alexander Stein,  
Nickias Kienle, Jakob B. Sørensen, and Dirk Fasshauer



**Fig. S1: Comparison of the displacement rates of the Alexa488-labeled synaptobrevin induced by different synaptobrevin layer mutants.**

Displacement is visible by a decrease in fluorescence anisotropy. About 100 nM of the  $\Delta$ N complex was incubated with different synaptobrevin mutants (500 nM). Note that displacement kinetics were very slow for  $\text{Syb}^{\text{I45A,M46A}}$  and  $\text{Syb}^{\text{N49A,V50A}}$ , whereas alanine double mutations in the coiled coil layers upstream of this region (i.e.  $\text{Syb1-96}^{\text{L32A,T35A}}$  and  $\text{Syb1-96}^{\text{V39A,V42A}}$ , corresponding to layers -7 & -6 and -5 & -4, respectively, Walter *et al.*, 2010) had a much less severe effect. The displacement speed induced by a synaptobrevin variant carrying an alanine point mutation in the C-terminal region ( $\text{Syb1-96}^{\text{F77A}}$ , layer +5, Walter *et al.*, 2010) was indistinguishable from wild-type synaptobrevin.

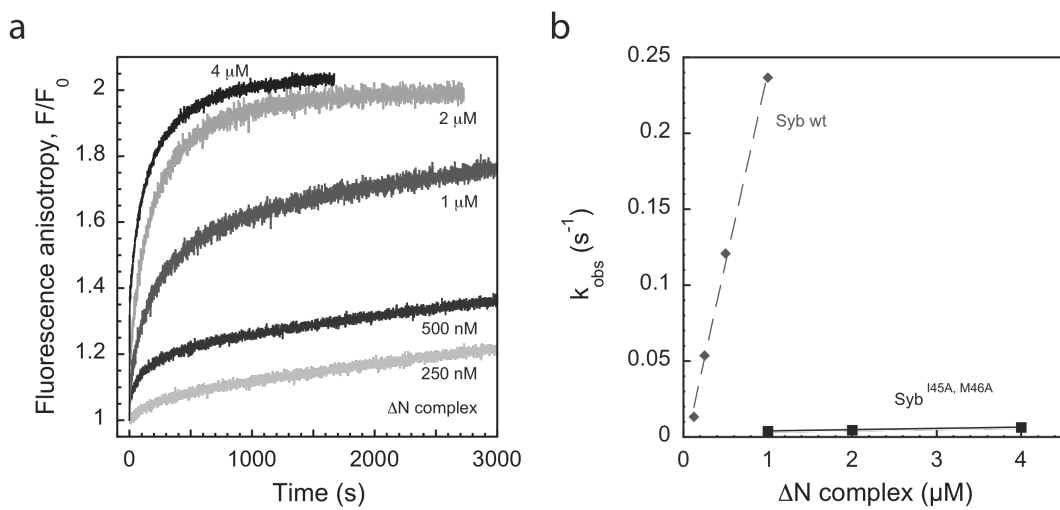


**Fig. S2: On-rate of Syb<sup>I45A, M46A</sup> binding to the  $\Delta N$  complex.**

a) The Alexa488-labeled synaptobrevin mutant Syb<sup>I45A, M46A, C28Alexa488</sup> binds to the  $\Delta N$  complex, which is indicated by an increase in fluorescence anisotropy. Syb<sup>I45A, M46A, C28Alexa488</sup> (100 nM) was mixed with the indicated amounts of purified  $\Delta N$  complex.

b) The pseudo-first order rate constants obtained from the single exponential fits of the reaction of Syb<sup>I45A, M46A, C28Alexa488</sup> and of wild-type Syb<sup>C28Alexa488</sup> (values taken from Walter *et al.*, 2010), with increasing amounts of  $\Delta N$  complex were plotted against the concentration of  $\Delta N$  complex. The slope of the linear fit yielded the on-rate of the reaction:  $\approx 860 \text{ M}^{-1} \text{ s}^{-1}$  for the double mutant and  $\approx 250,000 \text{ M}^{-1} \text{ s}^{-1}$  for wild-type synaptobrevin (Walter *et al.*, 2010). Note, that reactions using 250 nM and 500 nM  $\Delta N$  complex did not reach saturation and were therefore not included.

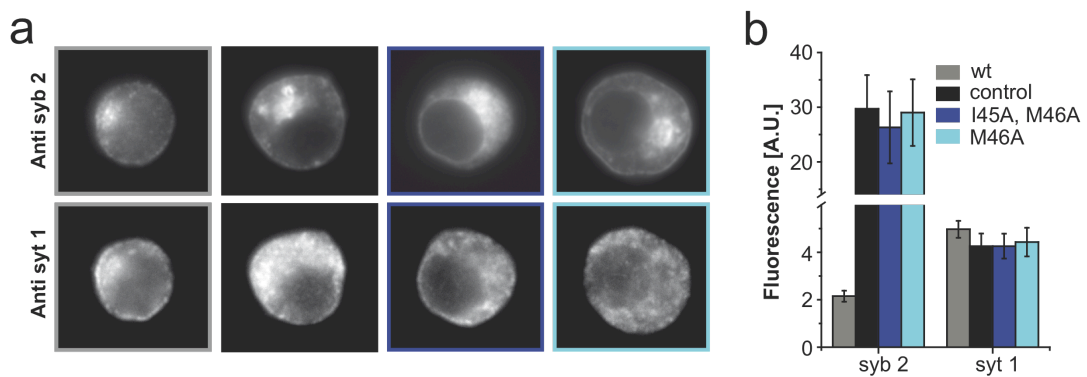


**Fig. S3: Immunostainings of overexpressed synaptobrevins.**

- a) Wide-field fluorescent images of stained and fixed wild-type chromaffin cells, either uninfected (wt) or virally expressing full-length synaptobrevin 2 (control), SybTMR<sup>I45A, M46A</sup>- or SybTMR<sup>M46A</sup> proteins. Top row: staining for Synaptobrevin 2 (syb 2), indicated by secondary antibody bearing Alexa546. Bottom row: staining for synaptotagmin 1 (syt 1), visualized by secondary antibody bearing Alexa647.
- b) Quantification of expression levels by fluorescence intensity (integrated fluorescence over the whole cell).

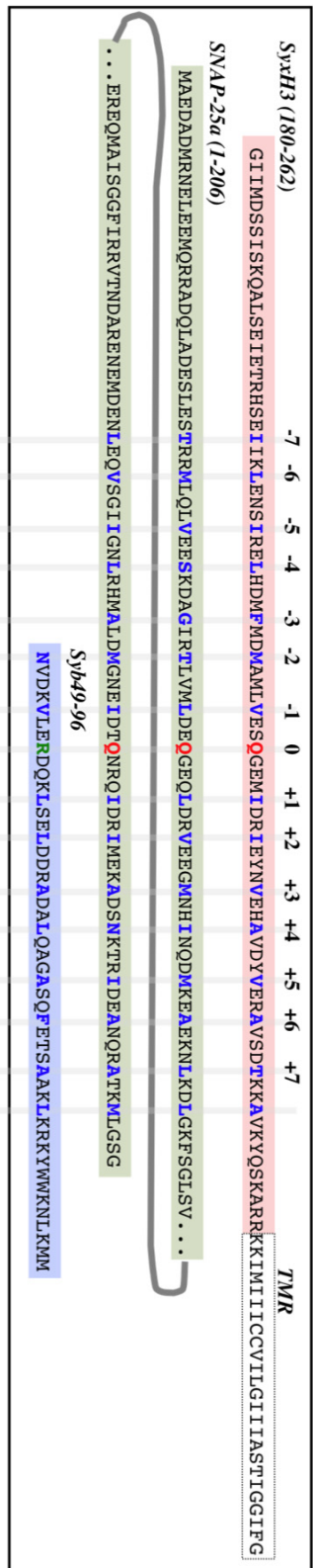


**Fig. S4: Schematic representation of the constructs and composition of the  $\Delta N$  complex used in the study.**

All constructs are shown by their amino acid sequence in single letter code. At the top, a box illustrates the composition of the  $\Delta N$  complex. The interacting coiled-coil layers, numbered from -7 to +8, are indicated. For binding experiments with soluble domains, a  $\Delta N$  complex was purified that contained the following SNARE protein constructs: SyxH3 (aa 180-262), full-length SNAP-25a (aa 1-206), and Syb49-96. For liposome fusion experiments, the  $\Delta N$  complex contained the SNARE motif of syntaxin 1a with the transmembrane region (SyxH3TMR, aa 183-288). Below, the constructs of the different R-SNARE homologs used for binding experiments are depicted. Arrows indicate the residues mutated in Syb1-96 and in endobrevin in this study. Dashed boxes indicate the putative trigger sequence region exchanged between tomosyn and synaptobrevin 2, and between tomosyn and endobrevin.

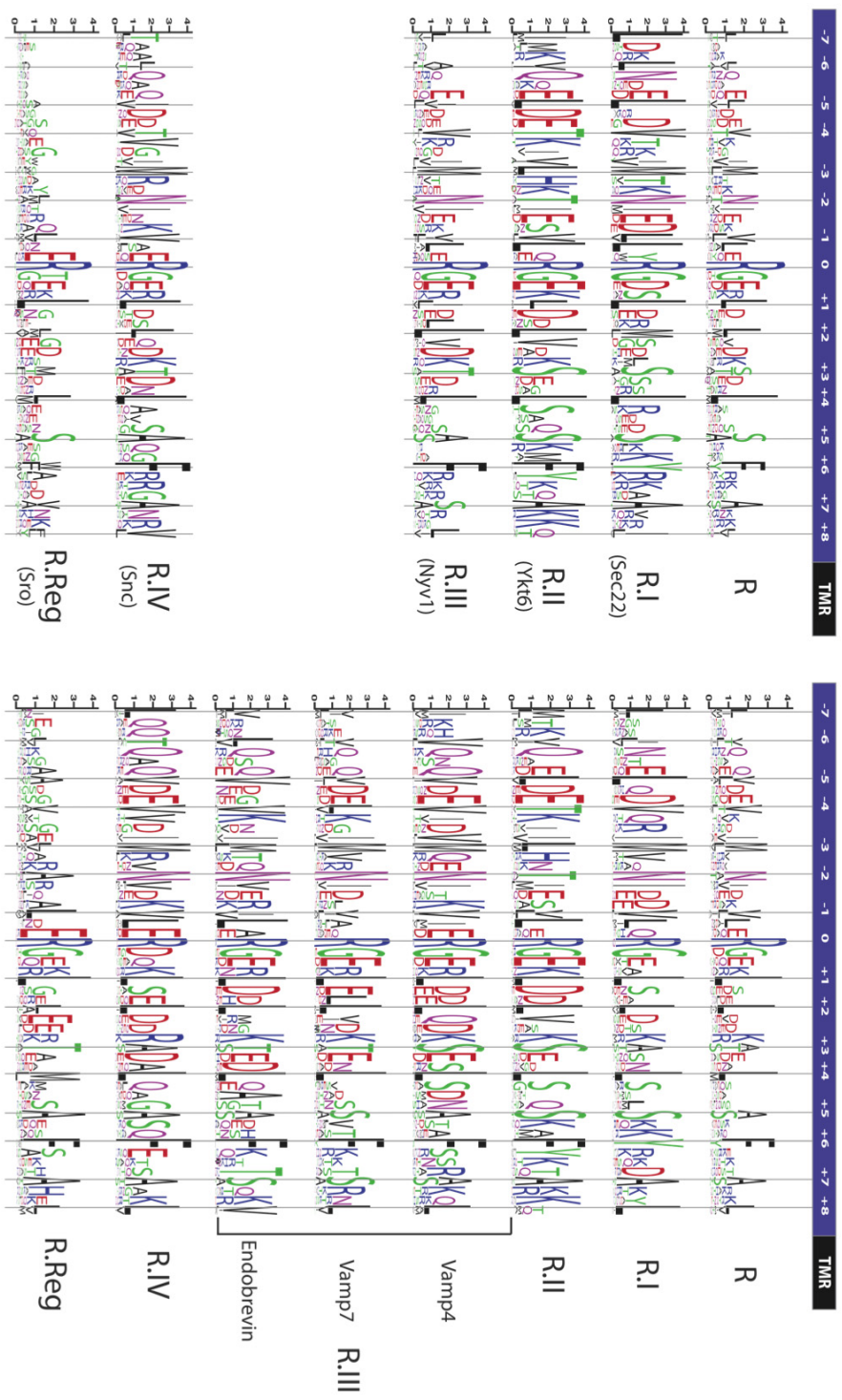


**Fig. S5: Conservation of the R-SNARE motifs in fungi and metazoans.**

We used the same approach as in Fig. 1 but divided the dataset into two subgroups. On the left hand side we included R-SNARE homologs only from fungi and on the right hand side those from metazoans only. In addition, we have further divided the metazoan R.III subgroup into the three basic groups: Vamp4, Vamp7, and endobrevin.